 MCB, vol.7, no.1, pp.45-58, 2010

Changes in Triphasic Mechanical Properties of Proteoglycan-Depleted Articular Cartilage Extracted from Osmotic Swelling Behavior Monitored Using High-Frequency Ultrasound

Q Wang[*], **YP Zheng**[*,†], **and HJ Niu**[*,‡]

Abstract: This study aims to obtain osmosis-induced swelling strains of normal and proteoglycan (PG) depleted articular cartilage using an ultrasound system and to investigate the changes in its mechanical properties due to the PG depletion using a layered triphasic model. The swelling strains of 20 cylindrical cartilage-bone samples collected from different bovine patellae were induced by decreasing the concentration of bath saline and monitored by the ultrasound system. The samples were subsequently digested by a trypsin solution for approximately 20 min to deplete proteoglycans, and the swelling behaviors of the digested samples were measured again. The bi-layered triphasic model proposed in our previous study (Wang et al., J Biomech Eng-Trans ASME 2007; 129: 413-422) was used to predict the layered aggregate modulus H_a from the data of depth-dependent swelling strain, fixed charge density and water content. It was found that the region near the bone, for the normal specimens, had a significantly higher aggregate modulus (Ha_1= 20.6 $\pm$ 18.2 MPa) in comparison with the middle zone and the surface layer (Ha_2= 7.8 $\pm$ 14.5 MPa and Ha_3= 3.6 $\pm$ 3.2 MPa, respectively) ($p < 0.001$). The normalized thickness of the deep layer $h_1$was 0.68 $\pm$ 0.20. After the trypsin digestion, the parametric values decreased to Ha_1 = 13.6 $\pm$ 9.6 MPa, Ha_2 = 6.7 $\pm$ 11.5 MPa, Ha_3 = 2.7 $\pm$ 3.2 MPa, and h_1 = 0.57 $\pm$ 0.28. Other models were also used to analyze data and the results were compared. This study showed that high-frequency ultrasound measurement combined with the triphasic modeling was capable of nondestructively quantifying the alterations in the layered mechanical properties of the proteoglycan-depleted articular cartilage.

Keyword: Articular cartilage, Ultrasound, Osmotic swelling, Biomechanics, Triphasic theory, Proteoglycan-depletion, Trypsin-digestion, Osteoarthritis

1 Introduction

Articular cartilage covers the articulating bony ends in diarthrodial joints to reduce the load on the bone and provide a frictionless and smooth surface for movement lubrication. Articular cartilage consists of a relatively small part of chondrocytes (5% of the total wet weight) and a large amount of extracellular matrix (ECM) (95%) rich in water, collagen fibres, proteoglycans (PGs), and other minor components (Mow et al., 2005). Different components of the tissue are interrelated and contribute to the layered structure. The depth-dependent distribution of these components and the organization of PGs and collagen fibres determine the mechanical properties of the tissue (Mow et al., 2005; Mankin et al., 2000).

Articular cartilage has been viewed as a biphasic material, composed of solid phase (PG-collagen matrix) and fluid phase (water and the dissolved ions) (Mow et al., 1980). The biphasic mixture theory has been applied in various experimental and theoretical studies on the mechanical properties of articular cartilage (reviewed by Mow et al., 2005; Mow and Guo, 2002). In view of the porosity and viscoelasticity of the tissue, the biphasic poroviscoelastic model was proposed (DiSil-

[*] Department of Health Technology and Informatics
[†] Corresponding author. Department of Health Technology and Informatics, The Hong Kong Polytechnic University, Kowloon, Hong Kong. Tel: 852 27667664; Fax: 852 23624365; Email: ypzheng@ieee.org
[‡] Department of Biomedical Engineering, The Beihang University, Beijing, China

vestro and Suh, 2002; Mak, 1986; Mak et al., 1987). Taking into account the electrical potential effects on the tissue including the fixed negative charges on PGs and the mobile ions in the matrix, the triphasic theory (Lai et al., 1991) was developed by researchers to describe articular cartilage as a triphasic material composed of solid, fluid and ion phases.

Swelling was described as an electrochemical mechanical coupling phenomenon of articular cartilage, arising from the interactions between the fixed negative charges and the mobile ions (Lai et al., 1991; Maroudas, 1976). Therefore, the negatively charged PGs would play an important role in the swelling behavior of articular cartilage. In comparison with other former theories, the triphasic theory more comprehensively describes the electrochemomechanism of swelling. Triphasic principles formulated the cartilage swelling with fixed charge density (FCD), water fraction, and the ion concentration (Lai et al., 1991; Narmoneva et al., 2001; Wang et al., 2007).

A homogeneous triphasic model was reported to predict swelling strains in articular cartilage with homogeneous modulus and Poisson's ratio (Lai et al., 1991; Setton et al., 1995). However, this homogeneous model could not describe the inhomogeneous properties of articular cartilage. Narmoneva et al. (2001) extended the homogeneous triphasic model to an inhomogeneous model with different aggregate moduli at the two layers of articular cartilage. But it should be regarded as a semi-inhomogeneous model due to a homogeneous modulus assumed in the deep layer. Considering the depth-dependent material properties of the entire cartilage layer, an improved inhomogeneous triphasic model developed in our previous study (Wang et al., 2007) was used to predict the aggregate moduli and swelling strains at different depths for the normal articular cartilage samples in the present study.

The bio-macromoleculars such as PGs and collagens might be degraded by proteolytic enzymes at the early- and mid-stages of cartilage degeneration (Sandy, 2003). The progressive degeneration of articular cartilage may lead to osteoarthritis (OA). As one of the dominant factors, the loss of PGs reportedly affected the swelling behavior of articular cartilage. Using MRI, Calvo et al. (2004) reported that there was a correlation between swelling (increment of cartilage thickness) and the PG depletion and cell loss. However, due to contrast problems and limits of spatial resolution, conventional MRI seems to have difficulty in accurately evaluating fine tissues such as articular cartilage. An optical method was designed to explore the variations of swelling strains and aggregate modulus of the OA cartilage from those of the normal cartilage tissue (Narmoneva et al., 2001, 2002). As only the cutting surface of the cartilage sample could be imaged, this optical method is 'destructive' and it was difficult to keep the specimen intact at the observed site.

High frequency ultrasound characterization of normal and OA articular cartilage has been the subject of many recent investigations since high frequency ultrasound has the advantages of high resolution, low-cost and being non-destructive, and it can provide morphological, acoustical, mechanical properties of the tissue. Many studies have reported on the changes in various acoustic parameters of the degenerated tissue, including the decrease of ultrasonic speed (Laasanen et al., 2002; Myers et al., 1995; Nieminen et al., 2002; Suh et al., 2001; Toyras et al., 1999), the increase of attenuation (Joiner et al., 2001; Nieminen et al., 2002), the reduction in reflection (Cherin et al., 1998, 2001; Laasanen et al., 2006; Nieminen et al., 2002), and the change of echo pattern (Hattori et al., 2005a, 2005b). In addition, ultrasound has been combined with indentation and compression for the measurement of tissue elasticity of degenerated cartilage (Fortin et al., 2003; Laasanen et al., 2002; Toyras et al., 1999; Zheng and Mak, 1996, Zheng et al., 2001, 2002, 2004a, 2005). However, few studies have been performed on the ultrasonic characterization of swelling behaviors when articular cartilage is degraded.

In our previous studies, the method of ultrasound combined with osmotic loading was applied to non-destructively measure the inhomogeneous swelling strains (Wang and Zheng, 2006) and the layered aggregate moduli (Wang et al., 2007) of the normal cartilage tissue; and the tis-

sue strain images during swelling was characterized (Zheng et al., 2006). It was found that the amplitude of the cartilage swelling decreased after trypsin digestion (Zheng et al., 2004b; Wang et al., 2008a). Based on the previous results, this study focused on the investigation of the changes in swelling behavior and mechanical properties of the PG-depleted articular cartilage. The ultrasound swelling measurement system (USMS) was used to obtain the swelling strains in situ and the bi-layered inhomogeneous triphasic model was applied to study the effects of PG-depletion on the mechanical properties of the cartilage matrix.

2 Materials and Methods

2.1 Specimen Preparation

Cartilage-bone plugs were prepared from fresh mature bovine patellae (n = 20) without apparent lesions by using a metal punch with a diameter of 6.35 mm (Wang and Zheng, 2006). Specimens were wrapped in wet gauze soaked with physiological saline and stored at -20°C until ultrasound examination. Before the test, each plug was cut into two parts (1/3 and 2/3) (Fig. 1a). The 1/3 portion was used as a control. The swelling behavior and trypsin digestion process of the 2/3 portion were monitored using ultrasound. Both trypsin-treated (the 2/3 portion) and control (the 1/3 portion) samples were assessed using histology and sectioned for water fraction measurement.

2.2 Ultrasound Examination

2.2.1 Acquisition system

The inhomogeneous swelling behavior and trypsin digestion of articular cartilage were monitored using an ultrasound swelling measurement system (USMS) developed in our laboratory (Fig. 1b) (Wang and Zheng, 2006; Zheng et al., 2004b). Ultrasound echoes reflected or backscattered from internal structures in the cartilage sample were collected by a 50 MHz ultrasound transducer (Model PI50-2, Panametrics, Waltham, MA, USA). Ultrasound signals were amplified by a pulser/receiver (Model 5601A, Panametrics, Waltham, MA, USA), and digitized by an 8-bit A/D converter at a sampling rate of 500 MHz (CompuScope 8500PCI, Gage, ON, Canada). A custom-designed program (Zheng et al., 2001, 2004b) was used to acquire and display data.

2.2.2 Swelling measurement

The prepared 2/3 portion of the cartilage sample was first thawed for three hours in physiological saline (0.15 M NaCl) at room temperature ($21\pm1^{\circ}$C). After that, the sample was mounted on the bottom of the container and fixed using rubber gel (Blu-Tack, Thomastown, Australia) (Fig. 1b). The outer ring ($\sim$ 0.6mm-wide) of the surface of the cartilage sample was gently covered by the rubber gel to ensure the diffusion of ions and water and the trypsin penetration into the cartilage sample from the surface layer toward the cartilage-bone interface.

In this study, the zero-swelling reference configuration was defined at 2 M NaCl, as the charge shielding was reportedly effective at hypertonic ion concentration and all swelling effects could be neglected (Eisenberg and Grodzinsky, 1985; Narmoneva et al., 1999a,b). The sample was first submerged in a 2 M saline solution for one hour to reach equilibrium. Then, the saline was rapidly (within 30 seconds) removed from the container using an injection syringe and replaced with physiological saline. The dynamic free swelling of the cartilage layer at different depths caused by the Donnan osmotic loading was observed in the ultrasound signals for one hour allowing the cartilage to reach equilibrium (Wang and Zheng, 2006; Wang et al., 2007; Zheng et al., 2004b).

The deformation of a cartilage layer at certain depth was extracted using a cross-correlation echo tracking method (Zheng et al., 2001; Ophir et al., 1999). The swelling strain was defined as the deformation over the original thickness of the layer (Wang et al., 2007). The experimentally measured strains at different depths would be used for triphasic modelling. The details of the calculation method have been introduced in our previous study (Wang et al., 2007).

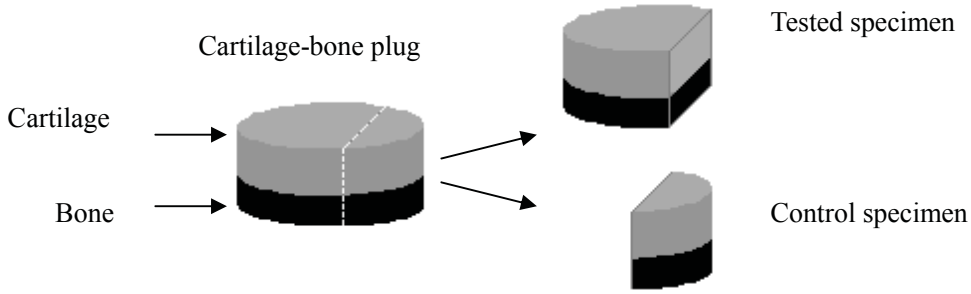

(a)

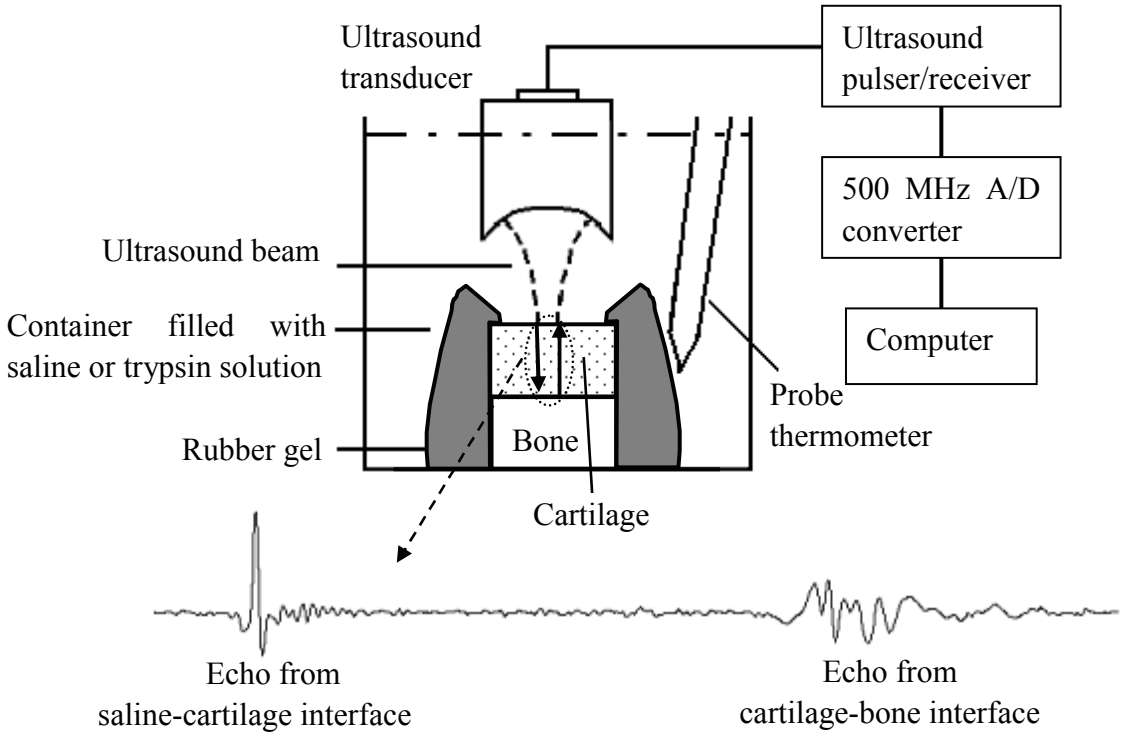

(b)

Figure 1: (a) Cartilage-bone plug was cut into two parts (1/3 and 2/3). (b) Schematic of the ultrasound experimental setup. Samples were mounted on the bottom of the container filled with saline or trypsin solution. A-mode ultrasound echoes from the cartilage tissue were acquired by the ultrasound system.

2.2.3 Enzyme digestion

After the swelling measurement, the 0.15 M NaCl solution was rapidly replaced with trypsin solution (0.25%, Cat. No. 25200-056, GiBCO, Invitrogen Inc., Burlington, ON, Canada). The specimens were immerged in the enzyme solution for approximately 20 minutes. The trypsin digestion was expected to obtain the PG-depleted cartilage samples. After digestion, the enzyme solution was further replaced with physiological saline. Due to the residual enzymes in the tissue, the digestion continued for three hours which was defined as the residual digestion phase (Wang et al., 2008b). During this phase, the digestion front formed by the interface of the digested and undigested cartilage tissue was observed in the M-mode ultrasound images in real-time (Fig. 2). The

M-mode ultrasound image was formed by drawing a line for each frame of ultrasound echo train as shown in Fig. 1b, where the gray level along the line indicates the amplitude of echo signal. As time going, a series of lines were drawn to form an M-mode image.

2.2.4 Swelling measurement of PG-depleted samples

The PG-depleted sample remained at the same position in the container after the digestion process. The aforementioned swelling measurement process was repeated. The specimen first equilibrated at the reference configuration, i.e. 2 M saline. Then, the bathing solution was changed back to the physiological condition, i.e. 0.15 M saline. The osmosis-induced swelling behavior of the degenerated cartilage was monitored and quantified.

2.3 Histological Evaluation

After the ultrasound examination was completed, both the control (the 1/3 portion) and PG-depleted specimens (2/3 portion) were cut into two parts, respectively. One part was used for histological evaluation and the other for water fraction measurement.

The parts for histological evaluation were fixed in 10% buffered formalin solution and quickly decalcified in 10% EDTA solution using an ultrasound-enhanced decalcification method (Guo et al., 2007). The serial tissue sections (4μm-thick) performed near the ultrasound-examined region, were stained with safranin O (SiGMA, CAT NO. F7258, USA) and contra-stained with fast green (SiGMA, CAT NO. S-2255, USA) (Leung et al., 1999). The sections were examined by a light microscopy imaging system including a microscope (model ECLIPSE 80i, Nikon, Japan) and a digital camera (DXM 1200X, Nikon, Japan). In optical micrographs, red color stained by safranin O indicated the presence of PG contents and the fast green-stained zone represented the PG-depleted cartilage layer (Leung et al., 1999; Qin et al., 2002).

2.4 Biochemical Analysis

2.4.1 Water fraction measurement

The full-thickness cartilage layer was serially sectioned into 5-7 layers with a thickness of approximately 200 μm. The slices were soaked in 2 M saline solution for one hour and the wet weight (WW_0) of each slice was measured. Then, the slices were equilibrated in 0.15 M saline for one hour, and dried at 37°C in an incubator for 12 hours. The dry weight (DW) of each layer was also measured. The ϕ_0^W in the reference configuration was calculated by Eq. (1) (Gu et al., 1996; Narmoneva et al., 1999b),

$$\phi_0^w = \frac{WW_0 - DW}{(WW_0 - DW) + DW(\rho_{2M}/\rho_s)} \tag{1}$$

where ρ_s, the density of the cartilage solid matrix, equals to 1.323 g/ml (Gu et al., 1996). ρ_{2M} denotes the density of the 2 M NaCl solution.

2.4.2 FCD Measurement

Since the dimethyl-methylene blue (DMMB) dye-binding assay could not be performed in our lab, an indirect method of image processing was designed to obtain the values of c_0^F based on the literature values. The averaged normalized distribution of hue (hue-saturation-value color map of the histological images) was calculated. Let each value $x_i = a_i x_{\max}$, where x_{max} is the maximum hue value, a is a coefficient, and i represents the number of the sub-layer which in this study was 1 to 9. Then, the integral area (A) of the hue distribution curve was a function of x, i.e. $A = f(x)$. Using the literature values of c_0^F as the reference (Narmoneva et al., 2001; Wang et al., 2002) (Fig. 3), the reference integral area was calculated as A_0. Assuming $A = A_0$, the relationship between the reference c_0^F and the hue values was obtained. Consequently, the calibrated c_0^F values were achieved.

2.5 Theoretical Triphasic Model

In this study, the triphasic theory (Lai et al., 1991) was used to predict the swelling strain mapping in articular cartilage. The tissue was modeled as a mixture of linear, isotropic, incompressible PG-collagen solid matrix and incompressible

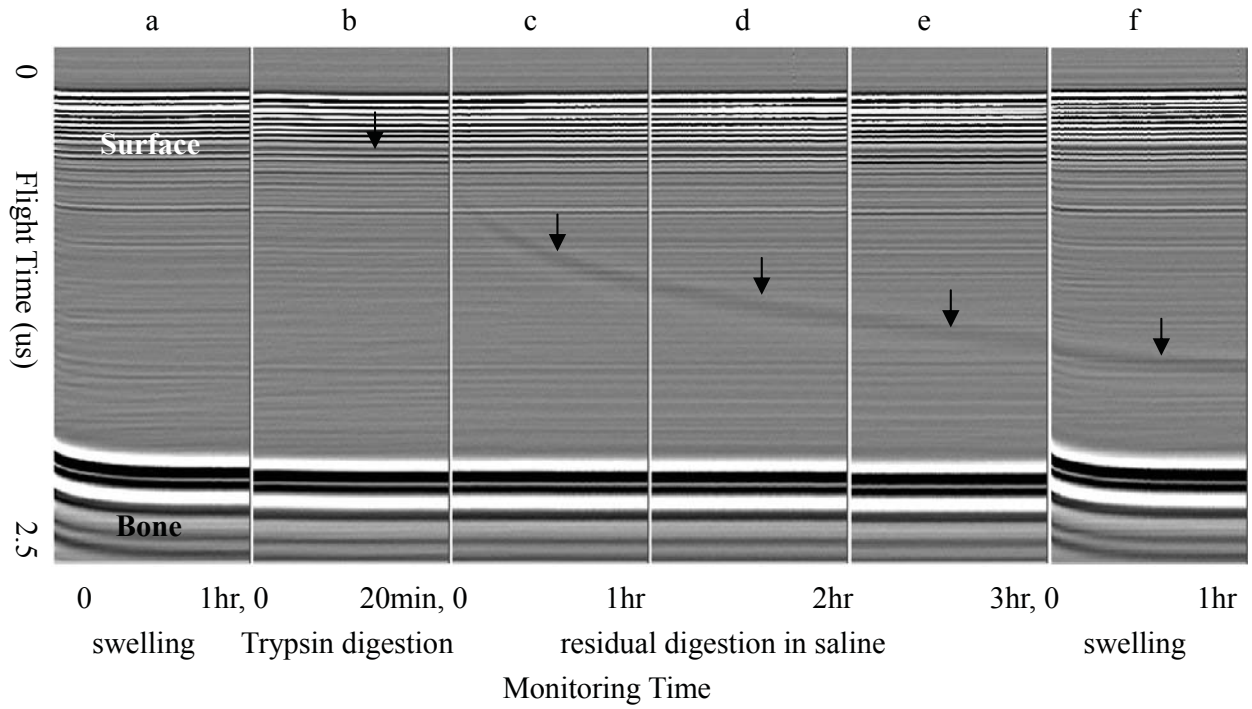

Figure 2: M-mode ultrasound images collected during different phases. (a) Swelling of the normal sample; (b) 20-minute trypsin digestion; (c-e) 3-hour residual digestion in physiological saline; (f) Swelling of the PG-depleted sample.

fluid consisting of water and ions. The cartilage-bone specimen was represented as the cylindrical triphasic material rigidly attached to the bone (Fig. 4). At the observation site of the central region with a diameter of ~ 0.1 mm, it was assumed that only axial deformations happened due to the osmotic loading.

In the free-swelling model, the interstitial fluid pressure (p) approximately equaled to the Donnan osmotic pressure related to the content of negatively charged PGs (FCD c_0^F), water volume fraction (ϕ_0^w), ion concentration (c^*) and the infinitesimal swelling strain tensor (E). The elastic stress on the cartilage solid matrix depended on the material and mechanical properties of aggregate modulus and Poisson's ratio. At equilibrium, all forces inside the tissue were balanced (Lai et al., 1991). Then the strains were predicted as a function of these biochemical, material and mechanical parameters and a geometric parameter of cartilage thickness (Wang et al., 2007).

In this study, the experimentally ultrasound-measured swelling strain data were inputted into a homogeneous model (Lai et al., 1991; Setton et al., 1995), Narmoneva's inhomogeneous model (Narmoneva et al., 2001) and our improved inhomogeneous model (Wang et al., 2007) (Fig. 4). The results were compared between the normal and PG-depleted cartilage samples using the statistical analysis software SPSS (V11.5, SPSS Inc., Chicago, US).

3 Results

3.1 Measurement of Water Fraction and FCD

The results of water fraction measurement showed no significant difference ($p > 0.5$, One-Way ANOVA) in the distribution of water content between the normal and trypsin- digested cartilage tissues (Fig. 5). While the FCD of the PG-depleted specimens significantly decreased ($p < 0.001$, One-Way ANOVA) (Fig. 6). The value of FCD in the deep layer was close to the normal value probably because the PGs in the deep layer were mostly not digested. It can be clearly observed in Figs 6b and 6c that trypsin digestion

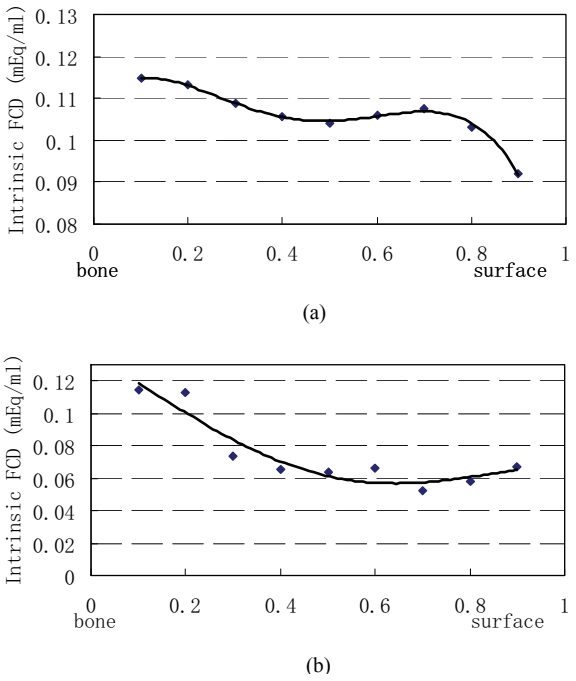

Figure 3: Depth-dependent distribution of fixed charge density (c_0^F) of (a) the normal cartilage (Wang et al., 2002) and (b) the degenerated cartilage (Narmoneva et al., 2001; Wang et al., 2002).

caused the lose of proteoglycan, which is labeled by safranin O in red.

3.2 Prediction of Aggregate Modulus and Swelling Strains

In our model, 4 parameters (Ha_1, Ha_2, Ha_3 andh_1) were predicted and compared with the corresponding parameters obtained using the semi-inhomogeneous model and the homogeneous model (Table 1). It was found that the region near the bone, for the normal specimens, had a significantly higher modulus (Ha_1= 20.6 $\pm$ 18.2 MPa) in comparison with the middle zone and the surface layer (Ha_2= 7.8 $\pm$ 14.5 MPa and Ha_3= 3.6 $\pm$ 3.2 MPa, respectively) (p < 0.001, ANOVA). The predicted thickness of the deep layer $h_1$was 0.68 $\pm$ 0.20, which indicates the separating location of the two layers with different changing rates of Ha. After the digestion, the Ha and $h1$ values decreased insignificantly (p > 0.15, ANOVA) to $Ha1$ = 13.6 $\pm$ 9.6 MPa, $Ha2$ = 6.7 $\pm$ 11.5 MPa, $Ha3$ = 2.7 $\pm$ 3.2 MPa, $h1$ = 0.57 $\pm$ 0.28. However, the

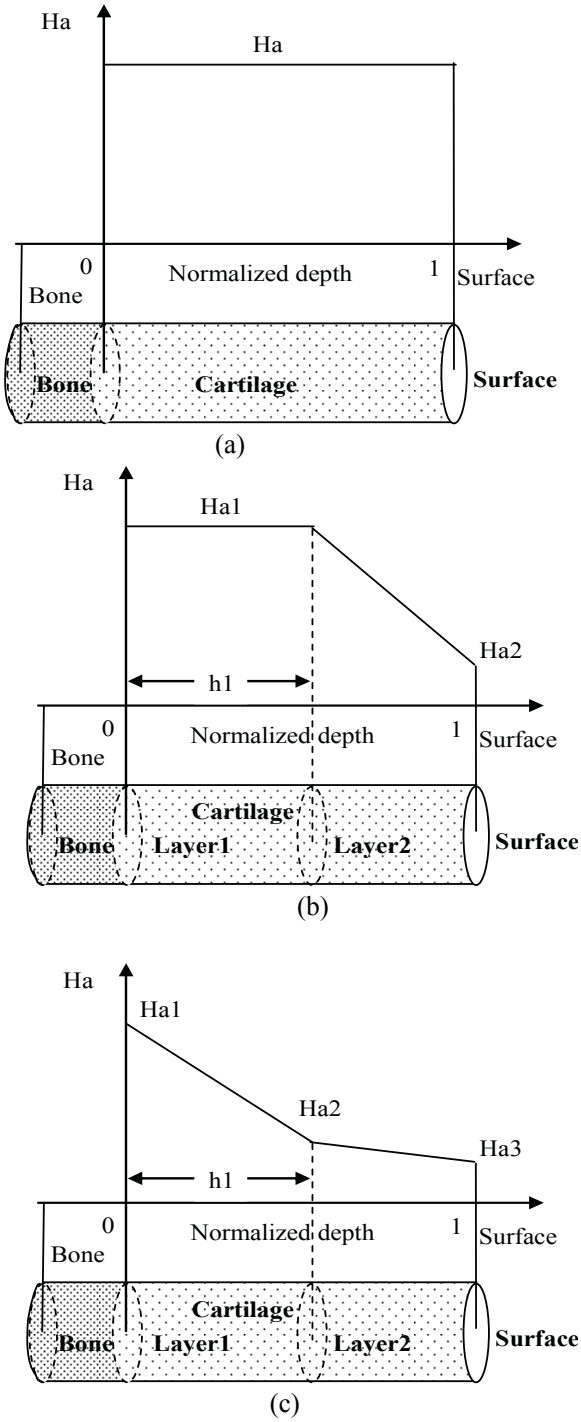

Figure 4: Schematic diagrams of the three triphasic models of articular cartilage used in this study. (a) Homogeneous model; (b) Semi-inhomogeneous model with 3 parameters (Ha_1, Ha_2, h_1) (Narmoneva et al., 2001); (c) Inhomogeneous model with four parameters (Ha_1, Ha_2, Ha_3, h_1) (Wang et al., 2007).

Table 1: The parameters (mean ± SD) predicted by the inhomogeneous model with 4 parameters in comparison with the results by the semi-inhomogeneous 3-parameter model and the homogeneous model.

Parameters	**4-parameter layered model**		**3-parameter layered model**		**Homogenous model**	
Normal (n = 20)						
Aggregate modulus (MPa)	Ha_1	20.6 ± 18.2	Ha_1	10.0 ± 14.9	Ha	4.7 ± 1.9*
	Ha_2	7.8 ± 14.5	Ha_2	3.3 ± 3.6		
	Ha_3	3.6 ± 3.2				
Thickness of Layer1 (mm)	h_1	0.68 ± 0.20	h_1	0.56 ± 0.26		
After trypsin digestion (n=20)						
Aggregate modulus (MPa)	Ha_1	13.6 ± 9.6	Ha_1	6.5 ± 10.1	Ha	3.2 ± 1.8
	Ha_2	6.7 ± 11.5	Ha_2	2.7 ± 3.6		
	Ha_3	2.7 ± 3.2				
Thickness of Layer1 (mm)	h_1	0.57 ± 0.28	h_1	0.50 ± 0.30		

* Significant difference ($p < 0.05$ by One-Way ANOVA)

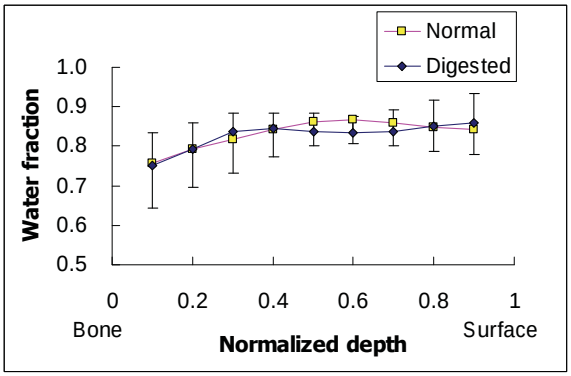

Figure 5: The depth-dependent distribution of water fraction (ϕ_0^w) of normal and PG-depleted articular cartilage. The error bars represent standard deviations (n = 20).

results showed that there was still significant difference ($p < 0.001$, ANOVA) among $Ha1$, $Ha2$, and $Ha3$, indicating the depth-dependence of aggregate modulus still existed. Fig. 7 shows the changes of the parameters of the specimens before and after trypsin digestion. The large standard deviation (error bars) indicated the large variations of parameters among different specimens. For both normal and digested specimens, it looks that the mean $Ha1$, $Ha2$ and $Ha3$ had a linear relationship, but this is not true for the results of individual specimens.

Similar results were obtained using the semi-inhomogeneous model (Narmoneva et al. , 2001) (Table 1). For both normal and digested samples, the aggregate modulus in the deep layer was insignificantly larger than that of the surface layer. $Ha1$ decreased from 10.0 ± 14.9 MPa to 6.5 ± 10.1 MPa, $Ha2$ from 3.3 ± 3.6 MPa to 2.7 ± 3.6 MPa, h_1 from 0.56 ± 0.26 to 0.50 ± 0.30, but all these changes are insignificant. The overall aggregate modulus Ha of normal specimens (4.7 ± 1.9 MPa) obtained using the homogeneous model (Setton et al., 1995) was significantly higher than that of the digested specimens (3.2 ± 1.8 MPa) ($p < 0.05$, ANOVA).

The depth-dependent swelling-induced strains of both normal and trypsin-digested articular cartilages were predicted. Fig. 8 shows the experimental result and theoretical prediction of the distribution of swelling strains across the depth of one typical sample of normal and PG-depleted articular cartilage, respectively. It was observed that the strains in the surface layer increased and the thickness (h_1) of the deep layer decreased due to PG depletion. However, the increase in the strains was not so apparent as that reported in Narmoneva's study for cartilage with OA (Narmoneva et al., 2001).

The normalized thickness of the undigested portion of the cartilage sample treated with trypsin

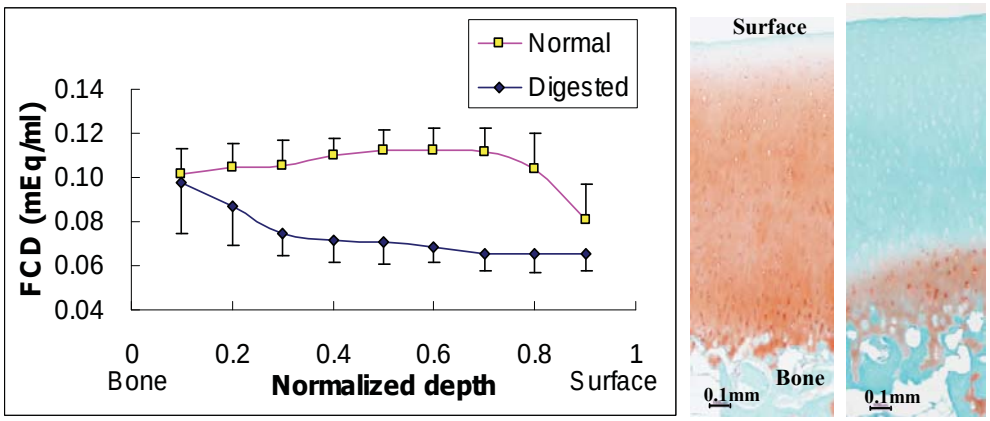

(a) (b) (c)

Figure 6: (a) The depth-dependent distribution of fixed charge density (c_0^F) and the histological sections of (b) normal and (c) PG-depleted articular cartilage. The error bars represent standard deviations (n = 20).

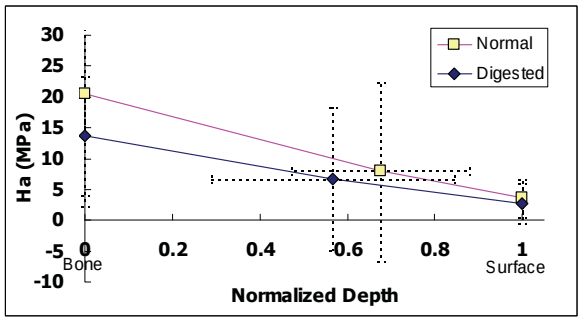

Figure 7: Comparison of parameters Ha_1, Ha_2, Ha_3, h_1 (mean $\pm$ SD) of the normal samples (n = 20) and the PG-depleted samples (n = 20).

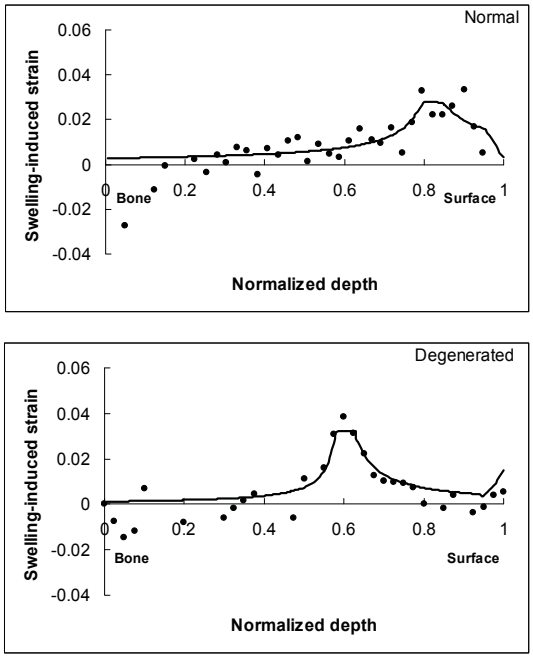

Figure 8: The inhomogeneous distribution of the swelling-induced strains of a typical cartilage sample for normal and PG-depleted articular cartilage. (a) Normal cartilage and (b) PG-depleted cartilage with 20-minute trypsin digestion. The solid lines in two figures represent the theoretical prediction of the strain distribution obtained using the inhomogeneous triphasic model (Wang et al., 2007).

was measured using both ultrasound and histology and compared with the value of h_1 predicted by our triphasic model. The normalized thickness of the undigested portion measured by ultrasound and histology was 0.32 ± 0.22 and 0.30 ± 0.15, respectively. The two measurements have a good agreement. However, no correlation was found between the thickness measured by ultrasound or histology with the value of h_1, which was decreased from 0.68 ± 0.20 to 0.57 ± 0.28. The issue would be discussed in the following section.

4 Discussion

This study predicted the aggregate moduli of articular cartilage at different depths using a

newly proposed 4-parameter layered model and the strain data obtained using ultrasound measurement. The results showed that the moduli of articular cartilage at different depths decreased after the PGs were depleted by trypsin digestion. These results were in general consistent with those in the literature and in particular those determined by a previous similar model (Narmoneva et al., 2001), where 3 parameters were used. However, the decreases of moduli obtained using the 4-parameter model ($Ha1$, $Ha2$, $Ha3$, h_1) as well as the 3-parameter model ($Ha1$, $Ha2$, h_1) used by Narmoveva et al. (2001) have not been demonstrated to be significant in the present study. This might be caused by the large variations observed among the results obtained from different specimens, i.e. the effects of trypsin digestion to different layers of cartilage tissues varied from specimen to specimen. However, the overall aggregate modulus Ha obtained using a model with single parameter (Setton et al., 1995) showed a significant decrease ($p<0.05$), indicating the whole cartilage tissue layer became softer after the trypsin digestion. It appears to conclude that while the overall stiffness of whole cartilage layer decreased significantly after trypsin digestion but each individual layers might show different patterns of changes for different specimens. The potential reasons for such phenomenon are further elaborated as follow.

It has been reported that trypsin digestion may cause a minor change in the tissue density (Gu et al., 1999) and in collagen network (Nieminen et al., 2002) in addition to the depletion of PGs. In this study, the PG-depleted cartilage samples did not show obvious changes in collagen fibrils according to the observation using polarized light microscope and in water fraction according to the measurement by weighting. These results might further suggest that the trypsin-induced PG depletion appeared to have insignificant effects on the stiffness of the matrix. In addition to the content of PGs, the stiffness of the cartilage matrix is also highly dependent on collagen fibers and water content. Narmoneva et al. (2001) suggested that the decrease of the modulus of OA cartilage was a result of the breakdown of collagen fibrils, the decrease of PGs and the increase of water. Meanwhile, Toyras et al. (1999) reported that a significant decrease of Young's modulus was found for both the collagen-damaged and PG-depleted cartilage samples. Different from this study, the enzyme of chondroitinase ABC was used to digest the PGs in their studies. Further experiments are needed to demonstrate whether trypsin and chondroitinase ABC would lead to different effects of PG-depletion on the reduction of the aggregate moduli in the degenerated cartilage. It should also be noted that the moduli were extracted using different models in these studies. Further studies are required to have a more detailed comparison for extracting mechanical properties by different models.

Similar values of the normalized thickness (h_1) of the deeper layer were predicted by the two bilayered triphasic models (Narmoneva et al., 2001; Wang et al., 2007). The finding that the value of h_1 decreased after digestion suggested that the PG depletion affected the layered structure of articular cartilage. Using Narmoneva's model, the value of h_1 of the PG-depleted cartilage was found to decrease from 0.56 ± 0.26 to 0.50 ± 0.30, which was consistent with the result reported by Narmoneva et al. (2001). To find the relationship between PG depletion and structural change, both histological assessment and ultrasound measurement of the thickness of the PG-remained cartilage layer were performed. However, it was found that the modeling results were much larger than those of histological and ultrasonic measurements. The difference demonstrated that the effect of the PG depletion on h_1 appeared not significant.

Moreover, there might be other possible affecting factors. Firstly, the relative insensitivity of our model to the extreme distributions of c_0^F and ϕ_0^W had been examined in our previous study (Wang et al., 2007). Secondly, the indirect method using image processing was designed to determine the values of FCD based on values measured using dimethyl-methylene blue in the literature (Narmoneva et al., 2001) and the hue-saturation-value distribution curve was obtained from our safranin O-fast green stained histological images. Al-

though the PG depletion could be quantified using safranin O-fast green staining (Kiviranta et al., 1987; Leung et al., 1999; Rosenberg, 1971), safranin O staining might make an overestimation of the loss of PGs. It was reported that the main components of PGs (chondroitin sulphate and keratan sulphate) were still detectable using biochemical method in the region of cartilage not stained by safranin O (Camplejohn and Allard 1988). In addition, it should be noted that only the color intensity but not true optical density might increase the uncertainty of the quantitative estimation of FCD. Thirdly, the experimentally measured swelling strain data of the PG-depleted cartilage were insignificantly changed in comparison with those of the normal cartilage. These data were used for theoretical parametric extraction, which might not be expected to obtain the significant variations in swelling strains. Narmoneva et al. (2001) measured the significantly changed swelling strain in the surface layer but found that the modulus in the surface layer of the OA cartilage was changed significantly in comparison with the normal cartilage. It should be noted that the specimens both before and after trypsin digestions were more intact in this study in comparison with Narmoneva's study, where cartilage was cut vertically and the cutting surface was monitored. The effect of cutting to the mechanical properties should be further studies.

It was found in this study that the depth-dependence of the osmosis-induced swelling strain of bovine patellar cartilage was similar to the results of the canine and human cadaver cartilage (Narmoneva et al., 1999b, 2001). Articular cartilage can be roughly separated into three zones: superficial, middle and deep zones, occupying approximately 10-20%, 40-60%, and 30% of the total tissue thickness, respectively (Mow et al., 2005). Each layer has different collagen fibrils orientation, cellular shape, and content distribution (Mow et al., 2005; Shapiro et al., 2001; Wang et al., 2002). The pattern of the swelling strain of articular cartilage is related to the distribution and orientation of different components. It has been known that the majority of the PGs are located in the middle and deep zones (Mow et al., 2005; Wang et al., 2002). Trypsin can cleave the PG aggregates and the PG fragments are released from the matrix causing the loss of PGs. It has been well documented that the loss of PGs will cause the significant reduction of tissue elasticity. In this study, it was observed that the partial PG depletion ($\sim$70%) altered the swelling strain of the degenerated cartilage tissue in the middle and surface layers. The strain in the deep zone changed insignificantly probably because the deep zone was almost not digested by trypsin, as confirmed by both the histological and ultrasound measurements.

5 Conclusion

In this study, the osmosis-induced swelling behaviors of both the normal and PG-depleted articular cartilage were investigated using our high-frequency ultrasound system. The results demonstrated that the ultrasonic measurement of the swelling-induced strains and the bi-layered inhomogeneous triphasic model could be used to extract the variations in the mechanical or geometric properties of the degenerated articular cartilage. The aggregate moduli and the thickness of the deep layer of the PG-depleted cartilage samples decreased insignificantly in comparison with those of the normal samples. The experimentally enzyme-treated OA-like cartilage only lost single or two compositions. However, the natural OA was a more complex process related to a multi-composition change of articular cartilage. Thus further studies are required to investigate the swelling behavior of the natural OA human articular cartilage using our ultrasound method.

Acknowledgement: This project was partially supported by the Research Grant Council of Hong Kong (PolyU5199/02E, PolyU5245/03E, PolyU5318/05E) and The Hong Kong Polytechnic University (1-BB69).

References

1. Calvo E, Palacios I, Delgado E, Sanchez-Pernaute O, Largo R, Egido J, Herrero-Beaumont G. 2004. Histopathological corre-

lation of cartilage swelling detected by magnetic resonance imaging in early experimental osteoarthritis. *Osteoarthritis Cartilage*. 12, 878-886.

2. Camplejohn KL, Allard SA. 1988. Limitations of safranin 'O' staining in proteoglycan-depleted cartilage demonstrated with monoclonal antibodies. *Histochemistry.* 89,185-188.

3. Cherin E, Saied A, Laugier P, Netter P, Berger G. 1998. Evaluation of acoustical parameter sensitivity to age-related and osteoarthritic changes in articular cartilage using 50-MHz ultrasound. *Ultrasound Med Biol.* 24, 341-354.

4. Cherin E, Saied A, Pellaumail B, Loeuille D, Laugier P, Gillet P, Netter P, Berger G. 2001. Assessment of rat articular cartilage maturation using 50-MHz quantitative ultrasonography. *Osteoarthr Cartilage.* 9, 178-186.

5. DiSilvestro MR, Suh JK, 2002. Biphasic poroviscoelastic characteristics of proteoglycan-depleted articular cartilage: Simulation of degeneration. *Ann Biomed Eng.* 30, 792-800.

6. Eisenberg SR, Grodzinsky AJ. 1985. Swelling of articular cartilage and other connective tissues: Electromechanochemical forces. *J Ortho Res.* 3, 148-159.

7. Fortin M, Buschmann MD, Bertrand MJ, Foster FS, and Ophir J. 2003. Dynamic measurement of internal solid displacement in articular cartilage using ultrasound backscatter. *Ultrasound Med Biol. J Biomechanics.* 36, 443-447.

8. Gu W, Lewis B, Lai WM, Ratcliffe A, Mow VC. 1996. A technique for measuring volume and true density of the solid matrix of cartilaginous tissues. *ASME Advances in Bioengineering* BED-33, 88-90.

9. Gu JD, Mao WY, Lai WM, Mow VC. True density of normal and enzymatically treated bovine articular cartilage. In: *Proceedings of 45th Annual Meeting of Orthopaedic Research Society*. Anaheim, CA. February 1–4, 1999. pp. 642.

10. Guo X, Zheng YP, Lam WL. 2007. Ultrasound machine assists decalcification. *Calcified Tissue Int.* 80, S52.

11. Hattori K, Ikeuchi K, Morita Y, Takakura Y. 2005a. Quantitative ultrasonic assessment for detecting microscopic cartilage damage in osteoarthritis. *Arthritis Res Ther.* 7, R38-46.

12. Hattori K, Takakura Y, Ishimura M, Tanaka Y, Habata T, Ikeuchi K. 2005b. Differential acoustic properties of early cartilage lesions in living human knee and ankle joints. *Arthritis Rheum.* 52, 3125-3131.

13. Joiner GA, Bogoch ER, Pritzker KP, Buschmann MD, Chevrier A, Foster FS. 2001. High frequency acoustic parameters of human and bovine articular cartilage following experimentally-induced matrix degradation. *Ultrason Imaging.* 23, 106-116.

14. Kiviranta I, Jurvelin J, Tammi M, Saamanen AM, Helminen HJ. 1987. Weight bearing controls glycosaminoglycan concentration and articular cartilage thickness in the knee joints of young beagle dogs. *Arthritis Rheum.* 30, 801-809.

15. Laasanen MS, Toyras J, Hirvonen J, Saarakkala S, Korhonen RK, Nieminen MT, Kiviranta I, Jurvilin JS. 2002. Novel mechano-acoustic technique and instrument for diagnosis of cartilage degeneration. *Physiol Meas.* 23, 491-503.

16. Laasanen MS, Toyras J, Vasara A, Saarakkala S, Hyttinen MM, Kiviranta I, Jurvelin JS. 2006. Quantitative ultrasound imaging of spontaneous repair of porcine cartilage. *Osteoarthr Cartilage.* 14, 258-263.

17. Lai WM, Hou JS, Mow VC. 1991. A triphasic theory for the swelling and deformation behaviors of articular cartilage. *J Biomech Eng.* 113, 245-258.

18. Leung KS, Qin L, Leung MCT, Fu LLK, Chan CW. 1999. Decrease in proteoglycans content of the remaining patellar articular cartilage after partial patellectomy in rabbits. *J Clin Exp Rheumatol.* 17, 597–600.

19. Mak AF. 1986. The apparent viscoelastic behavior of articular cartilage - the contributions from the intrinsic matrix viscoelasticity and interstitial fluid flows. *J Biomech Eng.* 108, 123-130.

20. Mak AF, Lai WM, Mow VC. 1987. Biphasic indentation of articular cartilage–I. theoretical analysis. *J Biomech.* 20, 703-714.

21. Mankin HJ, Mow VC, Buckwalter JA, Iannotti JP, Ratcliffe A. 2000. Articular cartilage structure, composition, and function. In: *Orthopaedic basic science*. 2nd edition. Buckwalter JA, Einhoun TA, Simnon SR. eds. American Academy of Orthopaedic Surgeons. pp. 444-470.

22. Maroudas A. 1976. Balance between swelling pressure and collagen tension in normal and degenerate cartilage. *Nature*. 260, 808-809.

23. Mow VC, Kuer SC, Lai WM, Armstrong CG. 1980, Biphasic creep and stress relaxation of articular cartilage in compression: Theory and experiments. *J Biomech Eng*. 102, 73-84.

24. Mow VC, Guo XE. 2002. Mechano-electrochemical properties of articular cartilage: their inhomogeneities and anisotropies. *Annu Rev Biomed Eng.* 4, 175-209.

25. Mow VC, Gu WY, Chen FH. 2005. Structure and function of articular cartilage and meniscus. In: *Basic Orthopaedic Biomechanics and Mechano-Biology.* 3rd edition. Mow VC, Huiskes R, eds. Lippincott Williams & Wilkins: Philadelphia, PA, USA. pp: 181-258.

26. Myers SL, Dines K, Brandt DA, Brandt KD, Albrecht ME. 1995. Experimental assessment by high frequency ultrasound of aticular cartilage thickness and osteoarthritic changes. *J Rheumatol.* 22, 109-116.

27. Narmoneva DA, Wang JY, Setton LA. 1999a. A new method for determination of the tensile modulus of articular cartilage in situ in a free swelling configuration. *ASME Adv. Bioeng.* BED-43: 31-32.

28. Narmoneva DA, Wang JY, Setton LA. 1999b. Nonuniform swelling-induced residual strains in articular cartilage. *J Biomech.* 32, 401-408.

29. Narmoneva DA, Wang JY, Setton LA. 2001. A noncontacting method for material property determination for articular cartilage from osmotic loading. *Biophys J.* 81, 3066-3076.

30. Narmoneva DA, Cheung HS, Wang JY, Howell DS, Setton LA. 2002. Altered swelling behavior of femoral cartilage following joint immobilization in a canine model. *J Orthop Res.* 20, 83-91.

31. Nieminen HJ, Toyras J, Rieppo J, Nieminen MT, Hirvonen J, Korhonen R, Jurvelin JS. 2002. Real-time ultrasound analysis of articular cartilage degradation *in vitro*. *Ultrasound Med Biol.* 28, 519-525.

32. Ophir J, Alam SK, Garra B, Kallel F, Konofagou E, Krouskop T, Varghese T. 1999. Elastography: ultrasonic estimation and imaging of the elastic properties of tissues. *Proc Inst Mech Eng.* 213, 203-233.

33. Qin L, Zheng YP, Leung CT, Mak AFT, Choy WY, Chan KM. 2002. Ultrasound detection of trypsin-treated articular cartilage: its association with cartilaginous proteoglycans assessed by histological and biochemical methods. *J Bone Miner Metab.* 20, 281-287.

34. Rosenberg L. 1971. Chemical basis for the histological use of safranin O in the study of articular cartilage. *J Bone Joint Surg Am.* 53(1), 69-82.

35. Sandy JD. 2003. Proteolytic degradation of normal and osteoarthritic cartilage matrix. In: *Osteoarthritis.* Brandt KD, Doherty M, Lohmander LS. eds. Oxford University Press, Oxford, New York. pp. 82-92.

36. Setton LA, Gu W, Lai MW, Mow VC. 1995. Predictions of swelling-induced pre-stress in articular cartilage. In: *Mechanics of Poroelastic Media.* Selvadurai, APS. ed. Kluwer Academic Publishers, Dordrecht. pp. 299-320.

37. Shapiro EM, Borthakur A, Kaufman JH, Leigh JS, Reddy R. 2001. Water distribution patterns inside bovine articular cartilage as visualized by 1H magnetic resonance imaging. *Osteoarthritis Cartilage*. 9, 533-538.

38. Suh JKF, Youn I, Fu FH. 2001. An *in situ* calibration of an ultrasound transducer: a potential application for an ultrasonic indentation test of articular cartilage. *J Biomech.* 34, 1347-1353.

39. Toyras J, Rieppo J, Nieminen MT, Helminen HJ, Jurvelin JS. 1999. Characterization of enzymatically induced degradation of articular cartilage using high frequency ultrasound. *Phys Med Biol.* 44, 2723-2733.

40. Wang CCB, Guo XE, Sun DN, Mow VC, Ateshian GA, Hung CT. 2002. The functional environment of chondrocytes within cartilage subjected to compressive loading: A theoretical and experimental approach. *Biorheology.* 39, 11-25.

41. Wang Q, and Zheng YP. 2006. Osmotic-induced shrinkage and swelling of normal bovine patellar articular cartilage *in situ* monitored using real-time high-frequency ultrasound. *Instrument Sci Technol.* 34, 317-334.

42. Wang Q, Zheng YP, Niu HJ, Mak AFT. 2007. Extraction of mechanical properties of articular cartilage from osmotic swelling behavior monitored using high frequency ultrasound. *J Biomech Eng-Trans ASME.* 129, 413-422.

43. Wang Q, Zheng YP, Leung G, Lam WL, Guo X, Lu HB, Qin L, Mak AFT. 2008a. Altered osmotic swelling behavior of proteoglycan-depleted bovine articular cartilage using high frequency ultrasound. *Phys Med Biol.* 53, 2537-2552.

44. Wang Q, Zheng YP, Qin L, Huang QH, Lam WL, Leung G, Guo X, Lu HB. 2008b. Ultrasonic assessment of progressive proteoglycan depletion of articular cartilage in real-time. *Ultrasound Med Biol.* In Print.

45. Zheng YP, and Mak AFT. 1996. An ultrasound indentation system for biomechanical properties assessment of soft tissues in-vivo. *IEEE Trans Biomed Eng.* 43, 912-918.

46. Zheng YP, Ding CX, Bai J, Mak AFT, Qin L. 2001. Measurement of the layered compressive properties of trypsin-treated articular cartilage: an ultrasound investigation. *Med Biol Eng Comput.* 39, 534-541.

47. Zheng YP, Mak AFT, Lau KP, Qin L. 2002. An ultrasonic measurement for *in vitro* depth-dependent equilibrium strains of articular cartilage in compression. *Phys Med Biol.* 7, 3165-3180.

48. Zheng YP, Bridal SL, Shi J, Saied A, Lu MH, Jaffre B, Mak AFT, and Laugier P. 2004a. High resolution ultrasound elastomicroscopy imaging of soft tissues: System development and feasibility. *Phys Med Biol.* 49, 3925-3938.

49. Zheng YP, Shi J, Qin L, Patil SG, Mow VC, Zhou KY. 2004b. Dynamic depth-dependent osmotic swelling and solute diffusion in articular cartilage monitored using real-time ultrasound. *Ultrasound Med Biol.* 30, 841-849.

50. Zheng YP, Niu HJ, Mak AFT, and Huang YP. 2005. Ultrasonic measurement of depth-dependent transient behaviors of articular cartilage under compression. *J Biomech.* 38, 1830-1837.

51. Zheng YP, Lu MH, Wang Q. 2006. Ultrasound elastomicroscopy using water jet and osmosis loading: Potentials for assessment for articular cartilage. *Ultrasonics.* 44(Supplement 1), e203-209.